Decadal variations in Labrador Sea ice cover and North Atlantic sea surface temperatures

Clara Deser and Marika Holland
Climate and Global Dynamics Division, National Center for Atmospheric Research, Boulder, Colorado, USA

Gilles Reverdin
Laboratoire d'Etudes in Géophysique et Océnographie Spatiales, GRGS, CNES, Toulouse, France

Michael Timlin
CIRES Climate Diagnostics Center, Boulder, Colorado, USA

Received 25 October 2000; revised 9 July 2001; accepted 13 September 2001; published 1 May 2002

[1] The spatial and temporal evolution of winter sea ice anomalies in the Labrador Sea and associated sea surface temperature (SST) variations in the North Atlantic are documented for three periods of above-normal ice cover: 1972–1974, 1983–1985, and 1990–1992. These events are notable for their winter-to-winter persistence, despite the fact that the ice margin retreats to northern Baffin Bay each summer, and for their spatial evolution, progressing from the northern Labrador Sea to the southern tip of Newfoundland over a 3 year period. Above-normal sea ice is consistently accompanied by below-normal SSTs in the subpolar Atlantic: the latter persist 1–3 years after the decay of the ice anomalies and in some cases exhibit a tendency for eastward movement across the gyre. Spring–summer freshwater anomalies at 100 m depth in the West Greenland Current are found to precede by ~8 months the initial occurrence of above-normal ice cover in the northern Labrador Sea. The role of atmospheric forcing in the joint evolution of anomalous sea ice and SST is assessed by means of an ice-ocean mixed layer model forced with observed air temperature and wind fields. The model results indicate that thermodynamic atmospheric forcing accounts for much of the winter-to-winter persistence and spatial evolution of the ice and concurrent SST anomaly patterns. However, the subsequent persistence of SST anomalies in the subpolar region is not well simulated, suggesting that oceanic processes omitted from the simple slab mixed layer formulation play a contributing role. *INDEX TERMS:* 3339 Meteorology and Atmospheric Dynamics: Ocean/atmosphere interactions (0312, 4504); 3349 Meteorology and Atmospheric Dynamics: Polar meteorology; 4540 Oceanography: Physical: Ice mechanics and air/sea/ice exchange processes; 9315 Information Related to Geographic Region: Arctic region; 9325 Information Related to Geographic Region: Atlantic Ocean; *KEYWORDS:* sea ice, decadal variability, North Atlantic Ocean, sea surface temperature, Labrador Sea

1. Introduction

[2] Sea ice is an integral component of the physical climate system, modulating surface albedo, turbulent air-sea energy exchange, and upper ocean stratification. Ice cover in the Labrador Sea exhibits substantial year-to-year variability, particularly during the winter season, as shown by *Walsh and Johnson* [1979], *Agnew* [1993], *Mysak and Manak* [1989], *Mysak et al.* [1990], *Chapman and Walsh* [1993], *Fang and Wallace* [1994], *Mysak et al.* [1996], *Slonosky et al.* [1997], *Prinsenberg et al.* [1997], *Parkinson et al.* [1999], and *Deser et al.* [2000a]. These studies document that winter ice variations in the Labrador Sea tend to be out of phase with those in the Greenland-Barents-Norwegian Seas. Such a configuration of sea ice anomalies has been attributed to a recurring large-scale pattern of atmospheric circulation changes broadly termed the North Atlantic Oscillation (NAO). It is likely that the prevailing positive polarity of the NAO in recent decades has contributed to the retreat of the winter ice edge in the Greenland-Barents-Norwegian Seas and to an advance in the Labrador Sea [cf. *Deser et al.*, 2000a].

[3] In addition to longer trends, decadal timescale fluctuations are prominent in many physical variables within the Labrador Sea, including upper ocean salinity, temperature, and sea ice [*Deser and Blackmon*, 1993; *Marko et al.*, 1994; *Houghton*, 1996; *Reverdin et al.*, 1997; *Belkin et al.*, 1998]. An intriguing lag association between decadal fluctuations in ice and sea surface temperature (SST) was reported by *Deser and Blackmon* [1993]. They found that periods of enhanced winter ice cover in the northern Labrador Sea tend to precede colder than normal SSTs east of Newfoundland by 1–2 years. Anomalous advection of cold, fresh water by the Labrador Current was suggested as a possible mechanism linking the ice and SST variations. Subsequent studies by *Houghton* [1996], *Reverdin et al.* [1997], and *Belkin et al.* [1998] investigated the horizontal and vertical structure of decadal-scale salinity and temperature fluctuations in the northern North Atlantic and slope currents of the Labrador Sea. Their results confirmed a propagating signal of cold, fresh anomalies from the Labrador Sea to the northeastern subpolar Atlantic in the upper several hundred meters, with a transit time (4–5 yrs) roughly consistent with the mean advection speed of the gyre. *Reverdin et al.* [1997] also found a

0148-0227/02/2000JC000683$09.00

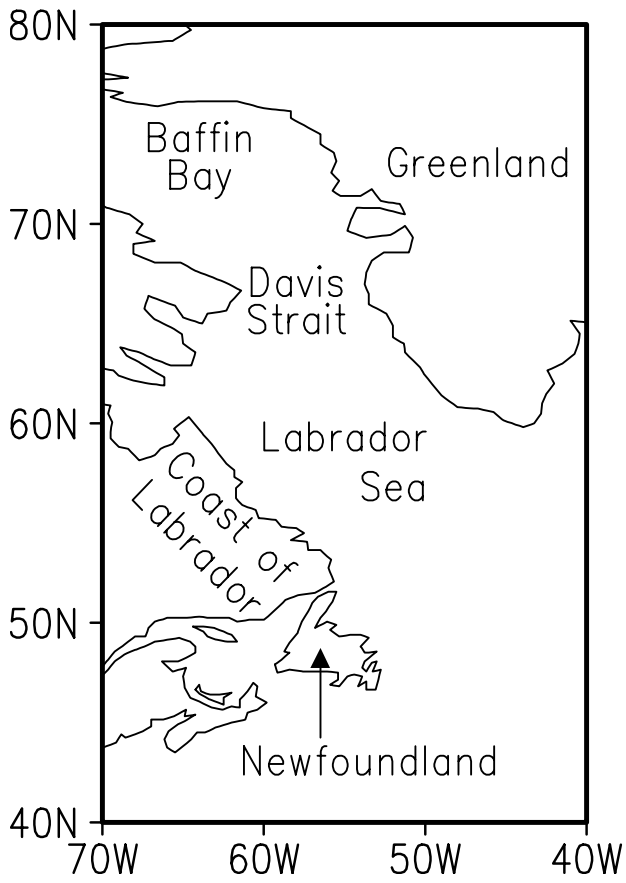

Figure 1. Geographical locations referred to in this study.

strong anticorrelation between ice cover and salinity fluctuations in the Labrador Sea and briefly noted that sea ice anomalies in the northern Labrador Sea tend to precede those in the south by 6 months to 1 year.

[4] The purpose of this study is to examine in greater detail the spatial and temporal evolution of decadal-scale sea ice anomalies in the Labrador Sea during winter. Is the southward progression noted by *Reverdin et al.* [1997] a robust feature? What is the role of atmospheric forcing in the evolution of anomalous sea ice cover? What is the nature of the lag association between sea ice and SST anomalies, and what is the role of atmospheric forcing in their coevolution? What is the temporal relation between sea ice and salinity anomalies within the Labrador Sea? To answer these questions, we perform simple analyses on gridded observational data sets of sea ice concentration, SST, and surface wind during 1953–1997. We also make use of a sea ice-ocean mixed layer model simulation forced by observed time-varying surface atmospheric fields. The data and analysis techniques are described in section 2. The observational and modeling results are reported in section 3 and discussed in section 4.

2. Data

[5] The sea ice concentration (SIC) data set is an updated version of that described by *Chapman and Walsh* [1993] containing end of month SIC values during 1953–1997. For this study the original 110 km equal area grid was interpolated to a 1° latitude by 1° longitude grid and smoothed in both the zonal and meridional directions with a three-point binomial filter. Thus only the gross features of interannual ice cover variability are resolved by our analyses. Further information concerning data sources and issues relating to homogeneity and quality control are given by *Chapman and Walsh* [1993, and references therein]. For a recent analysis of these data on a hemispheric scale, see *Deser et al.* [2000a].

[6] The SST data are from the Comprehensive Ocean-Atmosphere Data Set (COADS), an extensive archive of surface marine weather observations from merchant ships [see *Woodruff et al.*, 1987]. COADS data are quality-controlled but not corrected for changes in instrumentation and observing practice, and missing data are not filled in. The monthly mean data are archived on a 2° latitude by 2° longitude grid through 1997. We smoothed the monthly anomaly fields in both the zonal and meridional directions with a three-point binomial filter.

[7] Throughout this study the term "monthly anomaly" refers to the departure of a value for a given month from the long-term monthly mean. Seasonal anomalies are averages of the monthly anomalies. Unless stated otherwise, the statistical significance of correlation coefficients is assessed using a two-tailed Student's *t* test taking into account the effective number of degrees of freedom in the time series according to *Trenberth* [1984]. Only those correlations exceeding the 95% confidence level are discussed. A map of geographical sites referred to in this study is shown in Figure 1.

3. Results

3.1. Winter Sea Ice Variability

[8] The climatological distribution of SIC in the Labrador Sea during winter (December–March) is shown in Figure 2a. The marginal ice zone (concentrations between 0 and 100%) extends from the Davis Strait to the southwestern tip of Greenland and along the Labrador coast to Newfoundland. The interannual standard deviations of winter SIC (Figure 2b) are largest within the marginal ice zone, with maximum values ~22% directly south of the Davis Strait and 14% along the coast of Newfoundland.

[9] To define the dominant structure of interannual variability of ice cover in the Labrador Sea, we apply empirical orthogonal function (EOF) analysis to the area-weighted covariance matrix of winter SIC anomalies during 1953–1997. The leading EOF and its associated principal component (PC) time series are shown in Figure 3. The EOF, which accounts for 56% of the variance over the domain shown, is depicted in terms of the local correlation coefficient between the PC time series and the sea ice anomaly time series at each grid point. The EOF exhibits uniform polarity, indicating that winter sea ice anomalies tend to fluctuate in phase within the entire Labrador Sea (Figure 3a). Local correlation

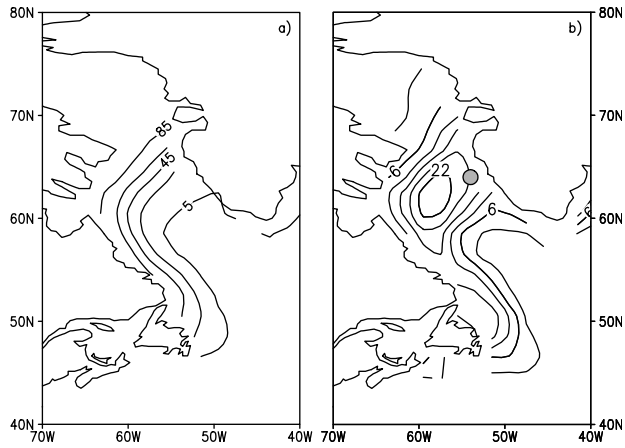

Figure 2. (a) Mean and (b) interannual standard deviation of winter (December–March) sea ice concentrations (percent) in the Labrador Sea based on the period 1953–1997. The contour interval is 20% (4%) for the mean (standard deviation) field. The circle in Figure 2b denotes the position of the Fylla Bank hydrographic station.

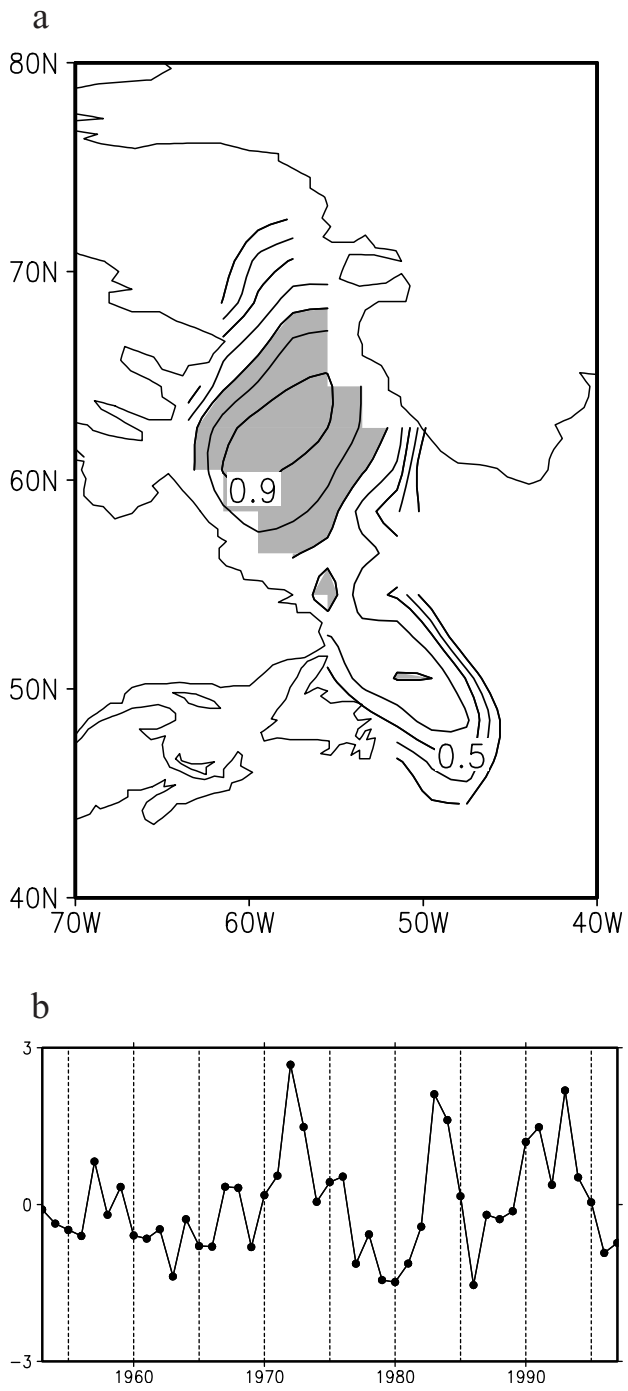

Figure 3. (a) Leading EOF of winter sea ice concentration anomalies in the Labrador Sea and (b) its PC time series. The EOF, which accounts for 56% of the variance over the domain shown, is depicted in terms of the local correlation coefficient between the PC time series and the sea ice anomaly time series at each grid point.

coefficients exceed 0.9 directly south of the Davis Strait and 0.7 off Newfoundland; that is, the EOF accounts for nearly all of the interannual variability in the Davis Strait and approximately half of the variability along the Newfoundland coast. The PC time series (Figure 3b) exhibits three distinct periods of extreme positive values (1972–1973, 1983–1984, and 1990–1993); a period of weaker positive values (relative to the years immediately before and after) occurs in 1957–1959.

[10] Sequences of sea ice anomaly maps for 1972–1974, 1983–1985, and 1990–1992 are shown in Figure 4. No temporal smoothing has been applied to these maps other than seasonal averaging. In 1972 the largest SIC anomalies are located south of the Davis Strait (values exceeding 50%), with weaker anomalies extending along the southern Labrador and Newfoundland coasts; this pattern closely resembles the EOF. In 1973, positive anomalies recur but with diminished amplitude in the Davis Strait and increased magnitude east of Newfoundland relative to 1972. In 1974, positive anomalies reappear off the southern tip of Newfoundland, with near-normal ice cover elsewhere. The ice anomaly sequences during 1983–1985 (Figure 4(middle)) and 1990–1992 (Figure 4(bottom)) exhibit many features in common with that during 1972–1974. Above-normal SIC occurs initially in the Davis Strait, followed in the next winter by a southward expansion and/or intensification of the positive anomalies along the southern coast of Labrador and in the third winter by positive anomalies off the Island of Newfoundland. It should be noted that sea ice retreats to northwestern Baffin Bay during the intervening summers (not shown).

[11] Two other periods of above-normal SIC are evident in the ice PC record: 1957–1959 and 1993–1994. The spatial evolution of winter SIC anomalies for these years is shown in Figure 5. Neither sequence conforms to the evolution of the three high ice events just shown. In particular, the positive SIC anomalies in 1957 are followed by near-normal conditions in 1958 and by weak positive anomalies in 1959. The positive SIC anomalies in 1993 are followed by weaker anomalies in 1994 (but no evidence for a southward expansion, although a distinct maximum occurs off Newfoundland) and near-normal conditions in 1995.

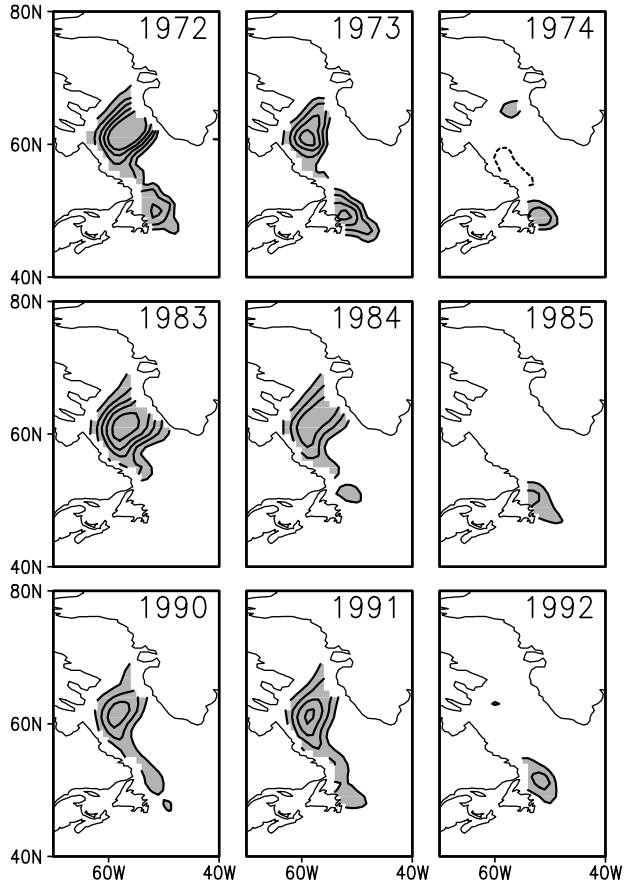

Figure 4. Sequences of winter sea ice concentration anomalies for three periods of high ice cover in the Labrador Sea. The contour interval is 5%; values >5% are shaded; the zero contour has been omitted; and the dashed contour is −5%.

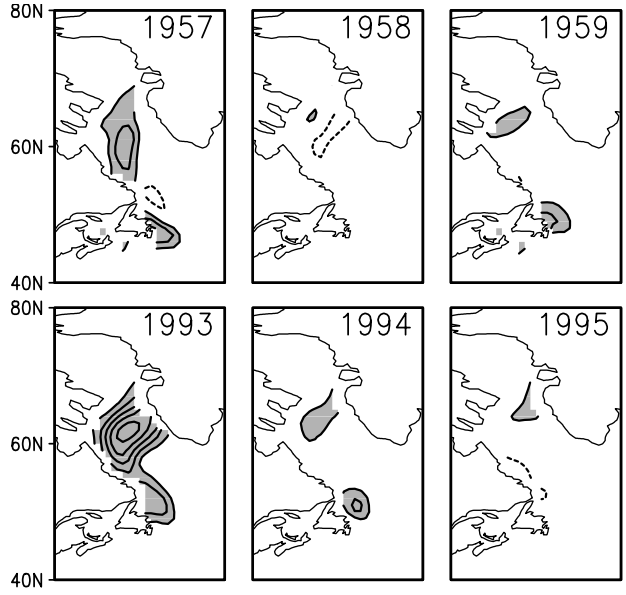

Figure 5. As in Figure 4 but for two additional periods of high ice cover.

[12] To document further the temporal relation between winter SIC anomalies in the northern and southern portions of the Labrador Sea, we constructed regional indices for the Davis Strait (58°–67°N, 64°–52°W) and for the area directly east of Newfoundland (45°–54°N, 54°–45°W); these records are shown in Figure 6. The Davis Strait ice index is nearly identical to the PC time series: its correlation coefficient is 0.98. The Newfoundland ice index tends to fluctuate in phase with and also lags the Davis Strait ice index, consistent with the results shown in Figure 4. This behavior is particularly evident during the periods of extreme ice cover in the 1970s, 1980s, and 1990s. The lag cross-correlation curve between the two records (Figure 7) confirms this tendency: maximum correlation coefficients (significant at the 99% confidence level) occur at zero and 1 year lag (0.73 and 0.77, respectively). The Newfoundland ice index exhibits higher persistence than the Davis Strait ice index, with a 1 year lag autocorrelation of 0.56 compared to 0.37.

3.2. Relation of Winter Sea Ice Variability to SST Anomalies in the North Atlantic

[13] One of the motivations for this study was to investigate further the link found by *Deser and Blackmon* [1993] between sea ice variations in the Labrador Sea and subsequent SST fluctuations in the subpolar North Atlantic. Here we present a composite analysis of the joint spatial and temporal evolution of winter SIC and SST anomalies associated with extreme ice conditions in the Labrador Sea. Figure 8 shows a sequence of lag correlation maps formed by correlating the leading ice PC (nearly identical results are obtained with the Davis Strait ice index) with the gridded SIC and SST anomaly fields at lags 0–3 years. The analysis is based on the period after 1965 to diminish the influence of the long-term SST cooling trend from the 1950s to the 1990s (see Figure 10) upon the correlations (beginning the analysis in 1961 or 1968 produces nearly identical results). SST anomalies are based on the extended cold season December–May in view of the strong persistence of winter SST anomalies through spring (not shown). Correlation values in excess of 0.30 (0.35) in absolute value are significant at the 95% confidence level for SIC (SST). For convenience we shall use the terms subpolar gyre (subtropical gyre) to refer to the portion of the North Atlantic Ocean poleward (equatorward) of ~45°N, just south of Newfoundland.

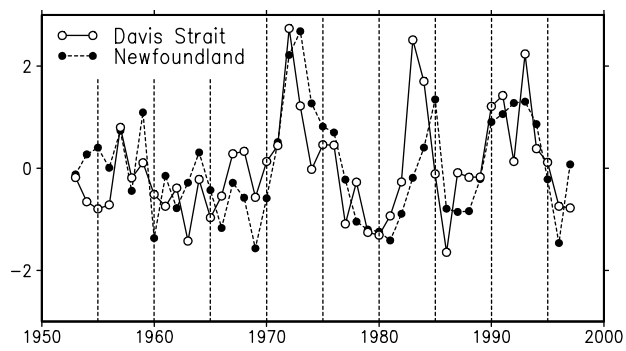

Figure 6. Regional winter sea ice concentration anomaly indices: Davis Strait (58°–67°N, 64°–52°W) (solid curve) and Newfoundland (45°–54°N, 54°–45°W) (dashed curve). Both curves are normalized by their respective standard deviations, and no temporal smoothing has been applied other than seasonal averaging.

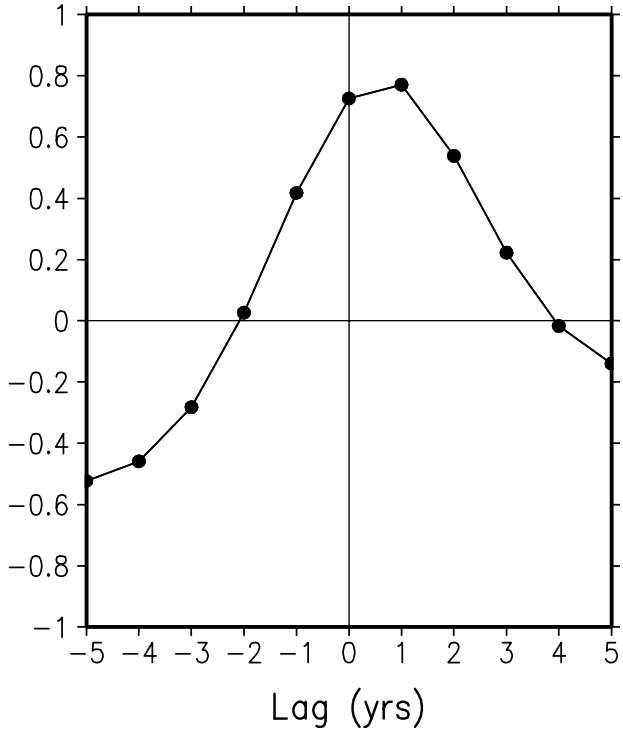

Figure 7. Lag cross-correlation curve between the Davis Strait and Newfoundland Ice Indices, based on data smoothed with a three-point binomial filter. Positive lags indicate Davis Strait leads Newfoundland.

[14] The sequence of lag correlation maps depicts a southward progression of SIC anomalies from the Davis Strait to Newfoundland over a 2 year period (lag 0 to lag 2), as expected from the results shown in section 3a. Negative SST anomalies in the subpolar gyre are associated with positive ice cover anomalies at all lags shown, with some evidence for an eastward progression over time (note that only the far eastern portion of the gyre contains significant correlations at lag 3 years). The SST patterns at lag 1 and 2 years, with negative values in the subpolar gyre and positive values in the western subtropical gyre, resemble the second EOF of winter SST anomalies shown by *Deser and Blackmon* [1993], confirming that their SST EOF is most closely associated with winter SIC anomalies in the Davis Strait 1–2 years earlier (note that Deser and Blackmon's study period ended in 1988).

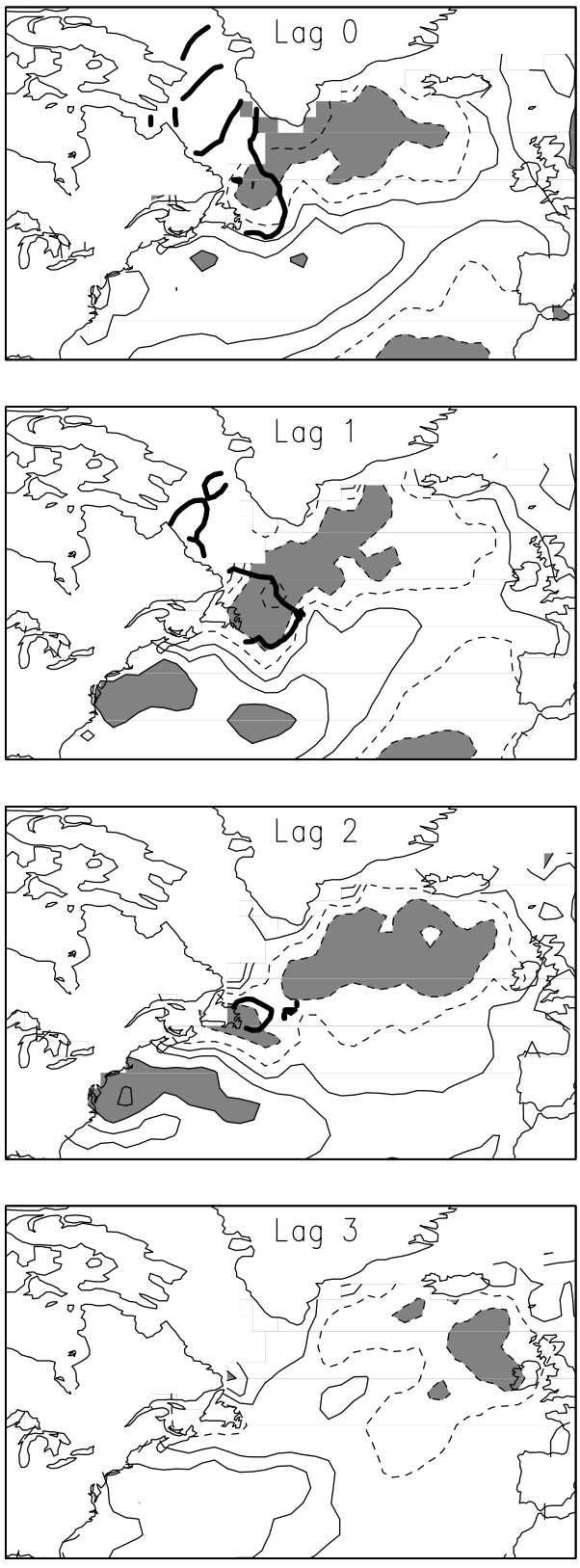

Figure 8. Lag correlation maps (lag in years) between the ice PC and winter anomaly fields of SST (thin contours) and sea ice concentration (thick contours) based on the period 1965–1997. The thin solid (dashed) contours denote positive (negative) SST correlations (contour interval = 0.2; zero contour is omitted); values ≤ -0.4 are shaded. Only the 0.4 and 0.8 contours are shown for the sea ice correlation fields.

[15] To what extent do individual high-ice events follow the composite evolution depicted in Figure 8? Joint sequences of winter sea ice and SST anomaly fields during 1972–1976, 1983–1987, and 1990–1994 are shown in Figure 9. Enhanced ice cover is consistently accompanied by below-normal SSTs over the western subpolar gyre in all the years shown, indicating that this aspect of the lag correlation analysis is robust. The persistence of negative SST anomalies 1–3 yrs after the decay of positive ice cover anomalies is also evident in many years, for example, 1974–1976, 1985–1987 (although we note that the SST anomalies in 1986 are more intense than those in 1985, suggesting more than simple persistence in this case), 1992, and 1994, confirming the lag correlation results. However, eastward movement of negative SST anomalies in the subpolar gyre is discernible only during 1972–1976 and 1990–1992, and positive SST anomalies near the Gulf Stream are evident only in 1983–1985 and 1993–1994: these aspects of the composite evolution are thus considered less reliable.

[16] The temporal association between sea ice anomalies in the Labrador Sea and SST anomalies in the subpolar North Atlantic is further illustrated in Figure 10, which shows the (inverted) Davis Strait ice index and the record of winter SST anomalies averaged over the eastern two thirds of the subpolar gyre (50°–62°N, 46°–12°W) where the lag 2 correlations in Figure 8 are strongest. No temporal smoothing has been applied to either record. As expected from Figure 9, below-normal SSTs accompany and persist 1–3 years beyond each period of severe ice conditions in the 1970s, 1980s, and 1990s. The weaker ice event in the late 1950s does not appear to be linked directly to below-normal SSTs, although a relative minimum in the SST index occurs in 1960–1963. A similar pair of curves was presented by *Deser and Blackmon* [1993; see also *Deser and Timlin*, 1996] for the period 1953–1988, although the indices are slightly different from those used here.

[17] The main results of section 3.1 and section 3.2 are summarized as follows. Three periods of anomalously high winter ice cover are identifiable in the Labrador Sea after 1953: 1972–1974, 1983–1985, and 1990–1994 (a weaker episode occurs in 1957–1959). The high-ice events during the winters of 1972–1974, 1983–1985, and 1990–1992 are notable for their persistence, despite the fact that the ice margin retreats to northern Baffin Bay each summer, and for their spatial evolution, progressing from the northern Labrador Sea to the southern tip of Newfoundland over a 3 year period. Positive ice cover anomalies are consistently accompanied by below-normal SSTs in the subpolar Atlantic and less consistently by positive SST anomalies in the western subtropical gyre. The subpolar SST anomalies persist 1–3 years after the decay of the ice cover anomalies and in some cases exhibit a tendency for eastward movement.

3.3. Relation of Winter Sea Ice Anomalies to Atmospheric Forcing

[18] Numerous studies have shown that anomalous atmospheric conditions play an important role in forcing anomalous winter SIC in the Labrador Sea [cf. *Ikeda et al.*, 1988; *Ikeda*, 1990; *Agnew*, 1993; *Fang and Wallace*, 1994; *Mysak et al.*, 1996; *Prinsenberg et al.*, 1997]. In particular, the strength of the northwesterly (offshore) surface geostrophic wind component and accompanying surface air temperature anomaly are strong determinants of winter sea ice conditions in the Davis Strait (Labrador and Newfoundland coasts). However, none of these studies explicitly examined the role of atmospheric forcing in terms of its contribution to the observed persistence and southward evolution of winter sea ice anomalies during the periods of enhanced ice cover in the 1970s, 1980s, and 1990s.

[19] Figure 11 shows the sequence of winter (December–February) geostrophic wind anomalies during 1972–1974, 1983–1985, and 1990–1992, superimposed upon the ice anomaly fields. The wind anomalies were derived from an updated version of the sea level pressure data set of *Trenberth and Paolino* [1980]

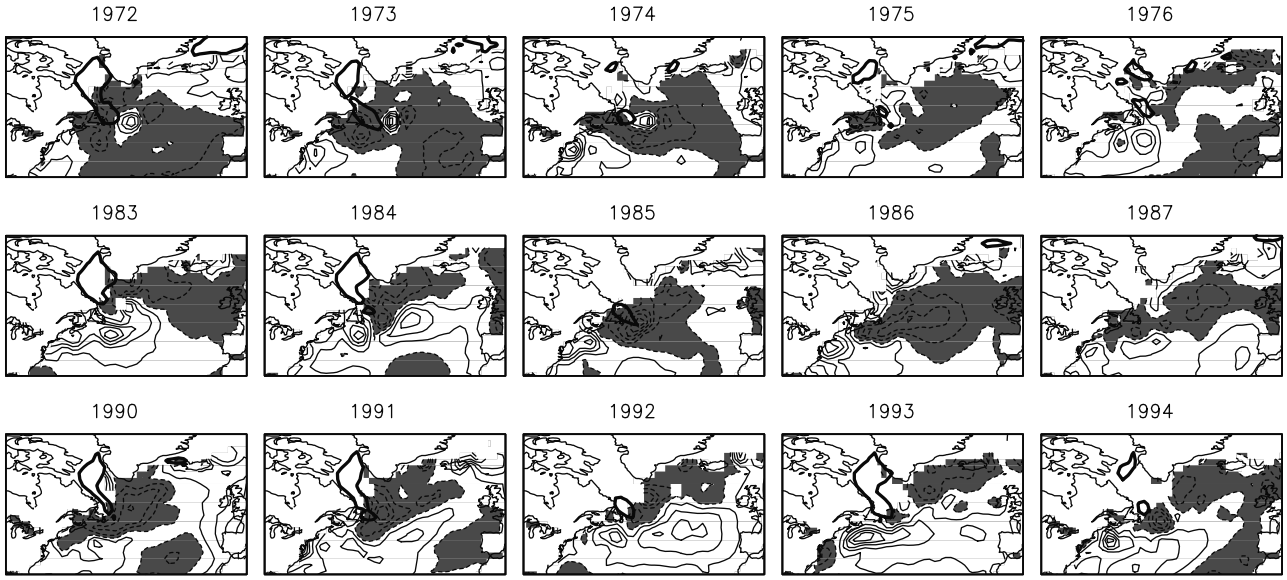

Figure 9. Sequences of winter sea ice concentration anomalies (thick contours) and SST anomalies (thin contours and shading) for three periods of high ice cover in the Labrador Sea. For sea ice, only the 10% isopleth is shown. For SST the contour interval is 0.35 K beginning at ±0.15 K, and solid (dashed) contours indicate positive (negative) anomalies, with values ≤ -0.15 shaded. Anomalies are with respect to the period 1965–1997.

archived on a 5° longitude by 5° latitude grid. In both 1972 and 1973 a coherent pattern of northwesterly geostrophic wind anomalies overlies the positive SIC anomalies in the Labrador Sea, while in 1974, anomalous offshore flow prevails over the region of enhanced ice cover directly east of Newfoundland. In 1983 and 1984, anomalous northwesterly flow occurs over the eastern portion of positive SIC anomalies in the northern Labrador Sea, while in 1985 the circulation is near-normal, although very weak offshore flow anomalies occur east of Newfoundland. The wind anomaly patterns over the Labrador Sea in 1990–1992 are similar to those in 1972–1974, with enhanced northwesterly flow over the extended ice margin in 1990 and 1991 and moderate offshore wind anomalies in the region of enhanced ice cover east of Newfoundland in 1992.

[20] These qualitative comparisons between the wind and ice anomaly fields lend support to the notion that atmospheric circulation conditions may be partially responsible for the observed spatial patterns and winter-to-winter persistence of positive SIC anomalies during 1972–1974 and 1990–1992, and to a lesser extent during 1983–1985. *Rogers et al.* [1998] have also documented the persistent nature of atmospheric circulation anomalies over the Labrador Sea during the early 1970s and mid-1980s, not only from winter to winter but extending into other seasons as well. The extent to which the southward evolution of positive SIC anomalies during the three episodes of high ice cover is attributable to atmospheric forcing is more difficult to assess from the general qualitative comparisons presented in Figure 11. For a more quantitative assessment of the role of atmospheric forcing we examine next a sea ice model simulation forced by observed surface atmospheric fields for the period 1948–1998.

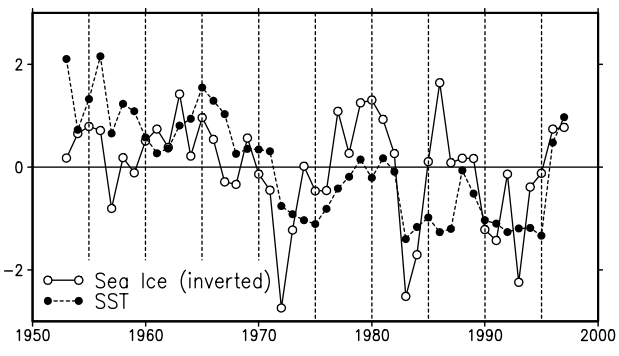

Figure 10. Winter Davis Strait ice index (inverted; solid curve) and SST anomalies in the subpolar North Atlantic (51°–61°N, 45°–13°W; dashed curve). Both records are normalized by their respective standard deviations, and no temporal smoothing has been applied other than seasonal averaging.

3.4. Sea Ice Model Simulation

[21] The model used in this study is an early version of the new sea ice component in the National Center for Atmospheric Research (NCAR) Community Climate System Model (CCSM), documented in full detail by B. P. Briegleb et al. (manuscript in preparation, 2002). It employs an elastic-viscous-plastic rheology [*Hunke and Dukowicz*, 1997] to solve the ice dynamics. This rheology approaches the viscous-plastic solution [*Hibler*, 1979] on the timescales associated with the wind forcing. A subgridscale ice thickness distribution [*Bitz et al.*, 2001] is used that allows for five ice and one open water category within each grid cell. This represents the high spatial variability present in the observed ice cover. The thermodynamics of each ice category is solved separately using the formulation of *Bitz and Lipscomb* [1999]. This results in different surface conditions for each category and thus different ice/atmosphere exchange. The ice model is run on a global grid that has the North Pole rotated into Greenland, allowing us to avoid the problem of converging meridians in the Arctic basin. The model resolution is 3.6° longitude by 1.8° latitude in the polar region.

[22] The sea ice model is coupled to a very simple slab mixed layer ocean model to allow for variable ocean temperatures and ice/ocean heat exchange. This slab model is not intended to be a physically complete formulation of the processes affecting ocean mixed layer temperatures but rather is meant to serve as a simple lower-boundary condition for the sea ice model. The mixed layer ocean model consists of independent columns beneath each grid cell in the ice model. The column

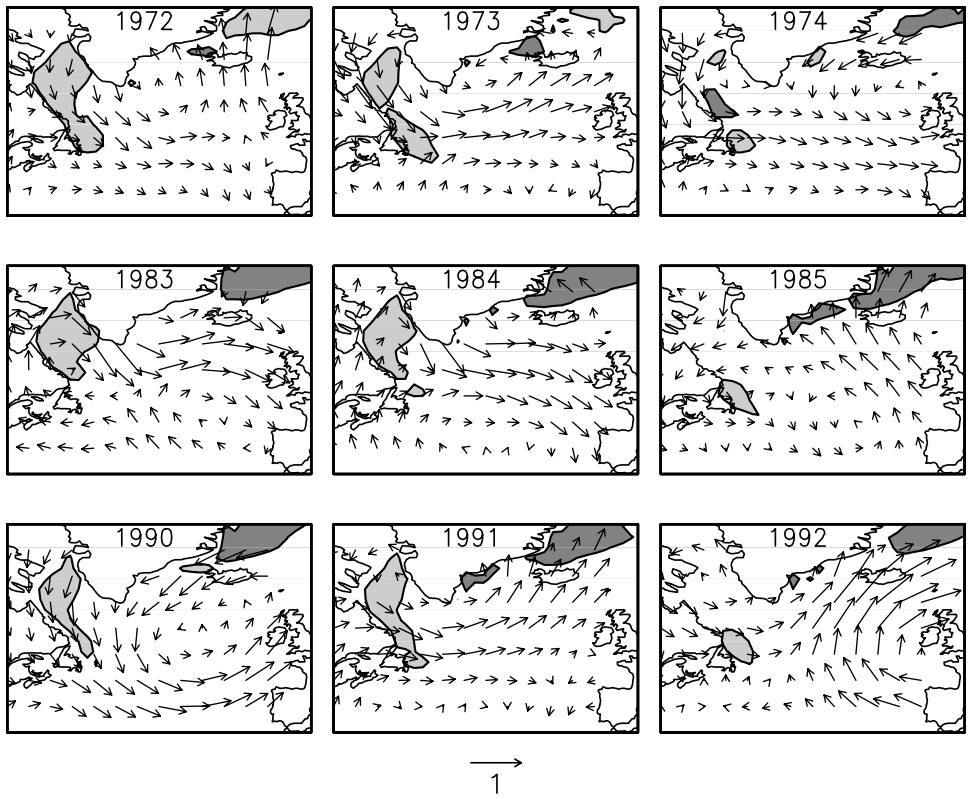

Figure 11. As in Figure 4 but for geostrophic surface wind anomalies. Ice anomalies >10% ($\leq -10\%$) are indicated with light (dark) shading.

depths vary seasonally as well as spatially, as described below. The governing equation for the T is

$$(\rho\, C_p\, H)\, dT/dt = Q_{\mathrm{atm}} + Q_{\mathrm{ice}} + Q_{\mathrm{ocn}}, \qquad (1)$$

where ρ is the density of seawater, C_p is the heat capacity of seawater, H is the mixed layer (column) depth, Q_{atm} is the sum of radiative (longwave plus shortwave) and turbulent (sensible plus latent) heat fluxes at the ocean-atmosphere interface, Q_{ice} is the ice-ocean heat exchange, and Q_{ocn} is the lateral and vertical oceanic heat exchange not explicitly accounted for in the slab ocean model (e.g., due to ocean currents, entrainment, etc.).

[23] The specifications of H, Q_{ocn}, and current velocities in the slab ocean model were obtained as follows. A separate "equilibrium" run was carried out with the ice model coupled to the ocean general circulation model component of CCSM (see *Smith et al.* [1992] for details of the ocean model). This coupled model was run for 100 years, forced by repeating cycles of observed 6 hourly surface atmospheric fields during 1984–1987 [*Large et al.*, 1997]. Mean annual cycles of H, Q_{ocn}, and current velocities at the top level of the ocean model were computed by averaging the data from the last 4 years of the 100 year integration. These quantities were then employed as lower-boundary conditions for the coupled ice slab ocean model integration used in this study. The simulated mixed layer depths and ocean current velocities in the North Atlantic are in reasonable agreement with observations (not shown).

[24] The coupled ice slab ocean mixed layer model used in this study is driven by observed interannually varying atmospheric forcing: specifically, near-surface air temperatures, humidities, and winds at 6 hourly resolution from 1948 to 1998 based on data from the National Centers for Environmental Prediction (NCEP)/NCAR Reanalysis Project [*Kalnay et al.*, 1986]. Climatological annual cycles of cloud cover and precipitation are specified on the basis of data from *Hahn et al.* [1987] and *Rossow and Schiffer* [1991], and *Xie and Arkin* [1996], respectively. A climatological annual cycle of shortwave radiation is computed according to *Bishop et al.* [1997]. Further details on the atmospheric conditions used to force the model are given by *Large et al.* [1997].

[25] The imposed wind and air temperature variations impact the distribution of sea ice thermodynamically through the surface turbulent energy fluxes, while the imposed wind stresses modify the ice through dynamical processes such as advection and ridging. An additional simulation is performed in which the air temperature is kept at a climatological annual cycle to isolate the role of direct dynamical wind forcing upon the sea ice field. In all simulations, ocean mixed layer salinity variations resulting from ice formation and melt do not feed back upon the sea ice distribution.

[26] It is important to note that in this simulation, sea ice anomalies may be advected by ocean currents, but the latter contain no interannual variability. Mixed layer temperature anomalies, on the other hand, cannot be advected by ocean currents since there is no lateral communication between adjacent grid cells in the ocean model (note that the effect of lateral and vertical ocean heat advection upon the mean annual cycle of mixed layer temperatures is implicitly accounted for by Q_{ocn}). It should also be noted that the formulation of the slab mixed layer model does not allow for any interannual "memory" in the ocean because of the neglect of physical processes such as entrainment and anomalous heat storage within the permanent and seasonal thermoclines.

[27] Figure 12 shows the modeled sequences of winter sea ice concentration anomalies during 1972–1974, 1983–1985, and 1990–1992, which may be compared to their observational counterparts shown in Figure 4. It is immediately apparent that the simulated ice anomalies are displaced south and east of the observed anomalies. This is due to an overly extensive climato-

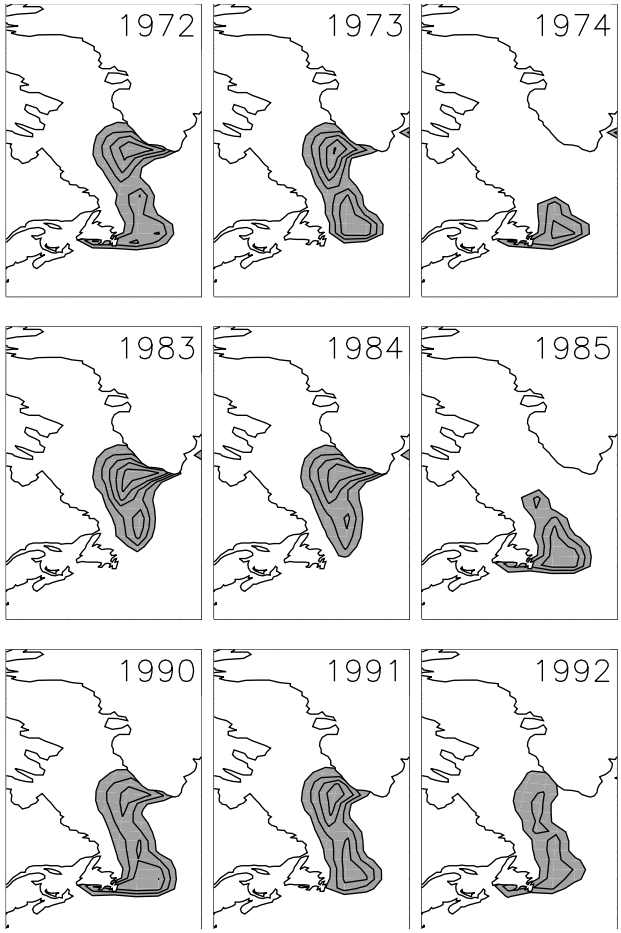

Figure 12. As in Figure 4 but for the standard model simulation.

logical mean winter ice cover in the model compared to observations (not shown). Despite the shift in position the modeled ice anomaly sequences bear a strong resemblance to observations, both in terms of amplitude and spatial pattern. For example, a positive ice anomaly extends from the southwest coast of Greenland to east of Newfoundland in 1972, followed by persistence of the anomaly in the north and enhancement of the anomaly in the south in 1973, followed by a single positive anomaly center east of Newfoundland in 1974. This sequence follows the observations closely. The evolution of ice anomalies during 1983–1985 is also similar to observations, although the southward expansion in 1984 relative to 1983 is less pronounced. The observed southward progression of positive ice anomalies during 1990–1992 is not well simulated, although the model is realistic in terms of persisting the high-ice conditions through all three winters.

[28] A further comparison of the model and observations is given in Figure 13, which shows the winter ice anomaly time series for the Davis Strait and Newfoundland regions. The correlation between the observed and simulated ice records is 0.77 for the Davis Strait and 0.72 for Newfoundland, indicating good overall agreement between the model and observations. In summary, the model simulates much of the observed winter-to-winter persistence and spatial evolution of the three main periods of enhanced ice cover in the Labrador Sea after 1953, suggesting that atmospheric variability is the main forcing for the sea ice anomaly patterns. This result is in keeping with the previous studies cited above.

[29] An additional simulation was performed in which the air temperatures are kept at their climatological annual cycles to isolate the role of direct dynamical wind forcing upon interannual ice cover anomalies. Strictly speaking, wind anomalies impact sea ice through both thermodynamic and dynamic processes; however, without the accompanying air temperature anomalies the thermodynamic effect of the wind anomalies is negligible compared to their dynamic influence (not shown). Comparing the simulations with full and "wind-only" forcing indicates that the direct dynamical effect of anomalous winds accounts for 8% (2%) of the simulated winter sea ice concentration anomalies in the Davis Strait (Newfoundland) regions. Thus, in this model, interannual variations in winter ice cover forced by atmospheric circulation anomalies are predominantly thermodynamically as opposed to dynamically driven. This result is consistent with the model simulations of *Ikeda et al.* [1988].

[30] As mentioned earlier, the surface wind and air temperature anomalies used to drive the sea ice model may themselves include a component due to air-sea interaction. In particular, the air temperature anomalies may implicitly contain a direct thermodynamic feedback from the sea ice anomalies (note that surface air temperatures in the NCEP reanalyses are determined prognostically over sea ice, with the presence of ice specified from the same observational archives used in this study). Thus, if in reality ice cover anomalies result from oceanic processes, their feedback upon surface air temperatures would be subject to misinterpretation in our model simulation. Additional experiments, such as a simulation that incorporates anomalous wind forcing advecting climatological air temperature gradients or one that couples an atmospheric boundary layer to the ice-ocean model, are needed to isolate the direct role of atmospheric thermodynamic forcing.

3.5. SST Simulation

[31] Although the ocean model used in this study is highly simplified, it is of interest to compare the simulated SST anomalies with observations. What aspects of the observed winter SST anomaly fields are consistent with the process of anomalous atmospheric forcing of a simple fixed depth slab mixed layer ocean? Figure 14 shows the lag correlation maps between the Davis Strait ice index and the SST anomaly fields from the model for lags 0–3 years (see Figure 8 for the maps based upon observations). At lag 0 the model correlation pattern is similar to observations, with negative values in the subpolar gyre and positive values in the western subtropical gyre, although the magnitudes are larger (we speculate that sampling fluctuations and intrinsic oceanic mesoscale variability reduce the signal-to-noise ratios and hence lower the correlations in the observed data). Unlike observations, the model correlations weaken with lag, and by the third year (lag 2), only the region directly east of Newfoundland contains significant negative correlations. Thus the simulated correlation map at a lag of 2 years deviates substantially from its observational counterpart, which exhibits robust negative correlations in the eastern two thirds of the subpolar gyre, in addition to a less consistent signal of positive correlations along the Gulf Stream. The differences in the lagged SST signal in subpolar gyre may reflect the contribution of oceanic processes not included in the simple slab ocean model. In particular, we conjecture that anomalous heat storage within the deep winter mixed layer, which can be reentrained during subsequent winters [cf. *Bhatt et al.*, 1998; *Watanabe and Kimoto*, 2000; *Deser et al.*, 2000b], coupled with advection of temperature anomalies by mean and anomalous ocean currents, may be important for prolonging SST anomalies in the subpolar gyre. Further simulations are planned with a full ocean general circulation model to evaluate this scenario.

3.6. Relation of Winter Sea Ice Variability to Upper Ocean Salinity Anomalies

[32] Evidence for decadal variations in upper ocean salinity at sites within the subpolar Atlantic has been presented by several

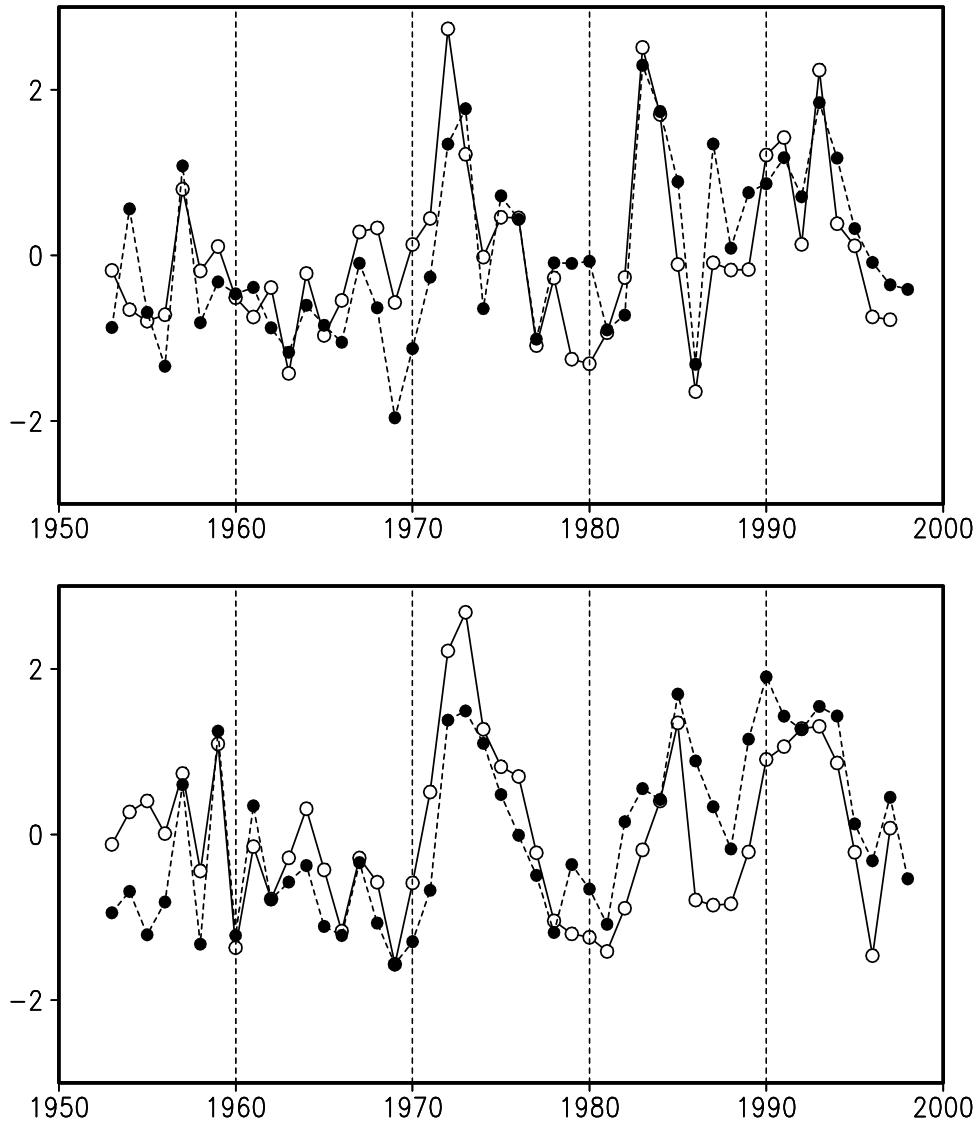

Figure 13. Observed (open circles) and simulated (solid circles) winter sea ice indices for (top) Davis Strait and (bottom) Newfoundland. All curves are normalized by their respective standard deviations, and no temporal smoothing has been applied other than seasonal averaging.

studies, including *Dickson et al.* [1988], *Houghton* [1996], *Belkin et al.* [1998], and *Reverdin et al.* [1997]. These studies support the notion of an advective pathway for freshwater anomalies from the Labrador Sea to the eastern subpolar gyre with a transit time of 4–5 years. *Reverdin et al.* [1997] also compared a spatially integrated measure of salinity anomalies in the subpolar gyre, which incorporates lag associations between the various sites, and winter ice conditions in the Labrador Sea. They found a strong out-of-phase relation between this spatially integrated salinity index and Labrador ice cover, such that periods of above-normal ice cover correspond to freshwater anomalies in the upper ocean and vice versa. Two interpretations were offered for this result: (1) low salinity in the Labrador Sea is directly (but not causally) associated with cold water flowing from the East Greenland Current or Canadian Arctic, which in turn is conducive to sea ice formation, and (2) low salinity contributes to the near-surface stratification and therefore winter surface cooling and ice formation [see also *Houghton*, 1996]. Here we report on the relation between winter SIC anomalies in the Davis Strait and salinity variations at 100 m depth in spring-summer (April–July; data in other months are not consistently available) off Fylla Bank (64°N, 54°W), which is located in the slope region influenced by the West Greenland Current (see Figure 2 for the location of Fylla Bank; the data sources are described by *Reverdin et al.* [1997]). Note that salinity variations at this site are coherent from 50 to 200 m depth (e.g., beneath the summer pycnocline) [*Reverdin et al.*, 1997].

[33] As shown in Figure 15, spring–summer freshwater anomalies off Fylla Bank tend to precede and sometimes also follow winters of above-normal ice cover in the Davis Strait during the 1950s, 1970s, 1980s, and 1990s. For example, below-normal salinity occurs in spring–summer of 1970 and 1971, while above-normal winter ice cover does not occur until 1972; these freshwater anomalies persist in spring–summer of 1972 and 1973, directly following winters of above-normal ice cover. Below-normal salinity also occurs in spring–summer of 1982 and 1989, ~6 months before the initial occurrence of above-normal winter ice cover; these freshwater anomalies then persist in spring–summer 1983 and 1990, respectively (data for 1991 are missing). Similar behavior is evident during 1993 and 1994 when freshwater anomalies follow positive SIC anomalies during the previous winter. Because salinity data are missing in 1956, we cannot determine whether low salinity leads the high-ice event in 1957–

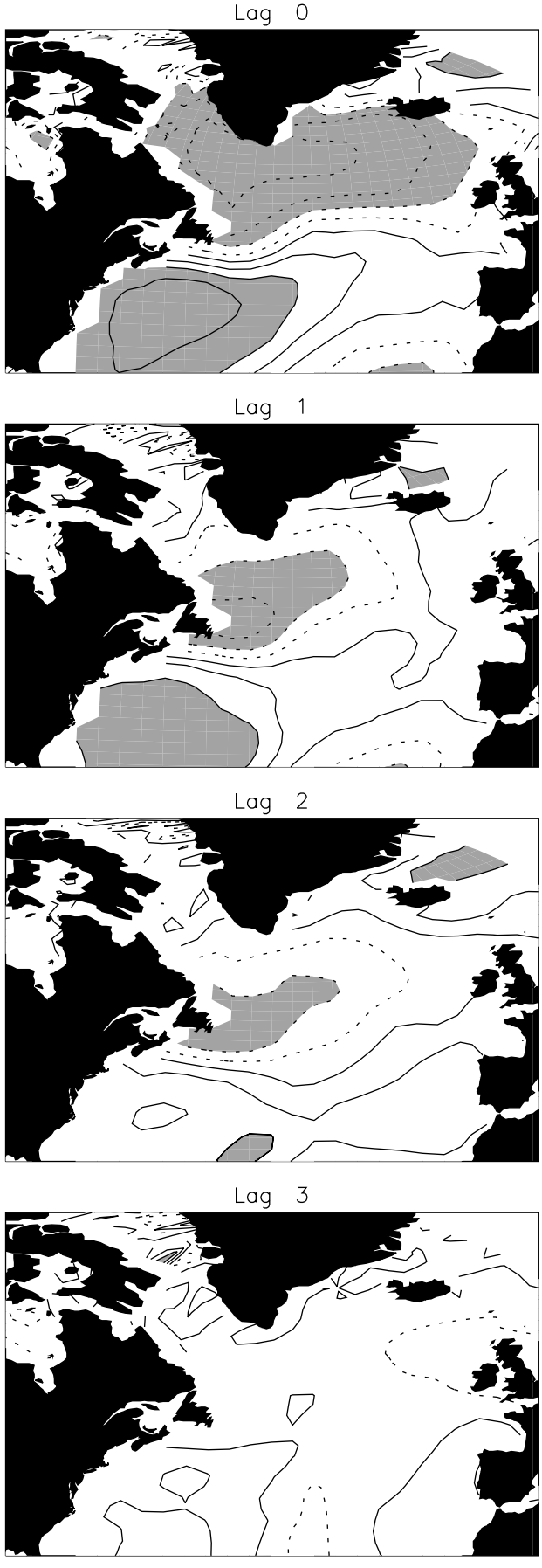

Figure 14. As in Figure 8 but for the model simulation.

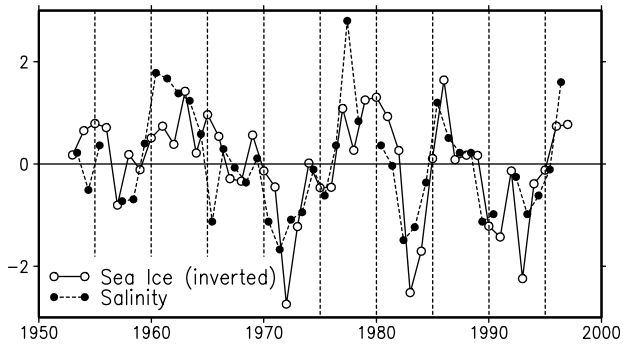

Figure 15. Inverted winter Davis Strait ice index (open circles) and April–July salinity anomalies at 100 m depth in the West Greenland Current (offshore of Fylla Bank; solid circles). Both curves are normalized by their respective standard deviations, and no temporal smoothing has been applied other than seasonal averaging.

1959; however, below-normal salinity follows above-normal SIC in spring–summer of 1957 and 1958.

[34] Figure 16 shows the lag cross-correlation curve between the sea ice and salinity records shown in Figure 15; negative (positive) lags indicate salinity leads (lags) sea ice. Note that the lags are offset from integer years because of the implicit 4 month lag between the April–July salinity record and the December–March ice index. The strongest negative correlations (significant at the 95% confidence level) are found at −20, −8, and +4 months, with a peak value of −0.83 at −8 months.

[35] A plausible physical interpretation of the results is that spring–summer upper ocean salinity anomalies precondition the water column for anomalous winter sea ice growth, as well as

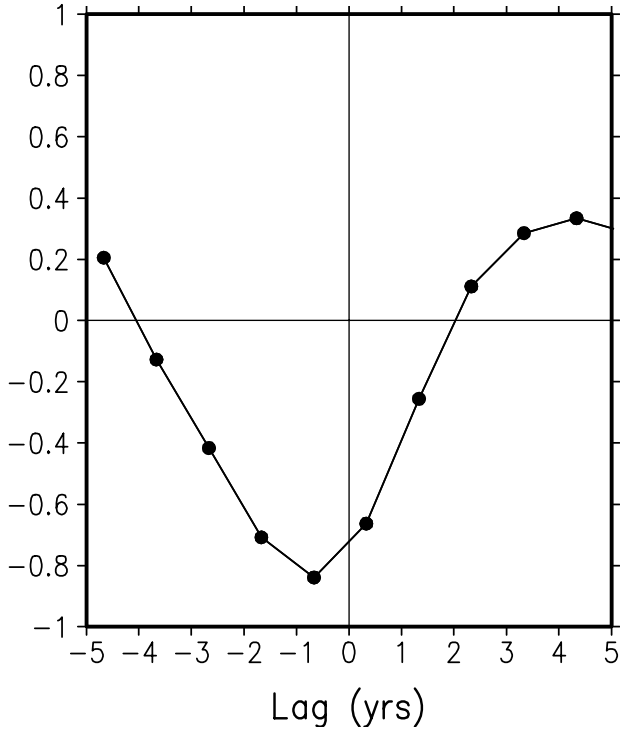

Figure 16. Lag cross-correlation curve between the Davis Strait ice index and the April–July salinity record at Fylla Bank based on data smoothed with a three-point binomial filter. Negative lags indicate the salinity record leads the ice index.

respond to anomalous local ice melt. Specifically, a freshwater anomaly, by stabilizing the upper ocean, may promote excess winter cooling, thereby facilitating sea ice growth, all other factors being equal. The enhanced winter ice cover will then freshen the upper ocean during the ensuing melt season. A similar conclusion was reached by *Marsden et al.* [1991], although their lag cross correlations were not as strong as those shown here [see also *Mysak et al.*, 1990; *Dickson et al.*, 1988]. However, as we have seen, atmospheric forcing appears to be the dominant factor controlling interannual sea ice variability in the Labrador Sea. Thus the apparent 8 month lead of freshwater anomalies relative to enhanced ice conditions may not necessarily reflect any causal connection; rather, we conjecture that anomalous large-scale atmospheric circulation conditions are responsible for both the salinity and the ice anomalies.

[36] Additional research is needed to understand the origin of upper ocean salinity anomalies off Fylla Bank in the West Greenland Current and their role, if any, in the development of enhanced winter sea ice cover in the Labrador Sea. The freshwater anomalies in 1970 and 1971 were likely due in part to the arrival of the "Great Salinity Anomaly," a freshwater pulse resulting from excess wind-driven export of Arctic sea ice through Fram Strait during the late 1960s, which was subsequently advected into the Labrador Sea by the East and West Greenland Currents [*Dickson et al.*, 1988]. The causes of the freshwater anomalies in 1982 and 1989 off Fylla Bank have not been definitively established: *Reverdin et al.* [1997] and *Belkin et al.* [1998] suggest that their origin may be local to the Labrador Sea/Baffin Bay region.

4. Summary

[37] We have described the evolution of winter ice conditions in the Labrador Sea during three periods of above-normal ice cover: 1972–1974, 1983–1985, and 1990–1992. These winter high-ice events are notable for their persistence, despite the fact that the ice margin retreats to northern Baffin Bay each summer, and for their spatial evolution, progressing from the northern Labrador Sea to the southern tip of Newfoundland over a three winter period. Although evidence was found for spring–summer freshwater anomalies at 100 m depth in the West Greenland Current to precede by ~8 months the occurrence of each period of above-normal winter ice cover, atmospheric conditions appear to play a determining role in the anomalous SIC distributions. In particular, each event of above-normal ice cover is accompanied by stronger than normal northwesterly winds within the Labrador Sea and offshore flow east of Newfoundland, consistent with the results of previous studies. A sea ice-ocean mixed layer model simulation was used to quantify the role of surface wind and air temperature forcing of the anomalous ice conditions during these three events. Surface atmospheric forcing was found to account for much of the persistence and spatial evolution of the anomalous ice conditions, with thermodynamic processes dominating over dynamical mechanisms. However, we caution that the use of observed air temperature anomalies (and to a lesser extent observed wind anomalies) to drive the ice-ocean model implicitly incorporates any direct thermodynamic feedback effects of the ice/SST anomalies upon the atmospheric boundary layer. Additional experiments in which variable wind forcing advects climatological air temperature gradients or a simulation in which an atmospheric boundary layer is coupled to the ice-ocean model are needed to isolate the direct role of atmospheric forcing upon sea ice cover.

[38] The observational results indicate that below-normal SSTs in the subpolar gyre accompany periods of enhanced ice cover. These SST anomalies persist 1–3 years after the decay of ice cover anomalies in the Davis Strait. The ice-ocean model simulates the concurrent association between ice cover anomalies in the Davis Strait and SST anomalies over the North Atlantic, suggesting that the joint ice/SST anomaly patterns are due to a common large-scale atmospheric forcing. However, the high persistence of SST anomalies in the subpolar gyre is not well simulated by the simple slab ocean mixed layer model. This shortcoming may indicate that oceanic processes not included in the model, such as horizontal advection and the seasonal cycle of vertical entrainment through the base of the mixed layer that can tap the anomalous heat stored at depth, contribute to the observed SST persistence characteristics. Comparison of the slab ocean mixed layer simulation to an ocean general circulation model is required to test these ideas.

[39] **Acknowledgments.** This study was supported in part by grants from NSF Physical Oceanography Atlantic Circulation and Climate Experiment to C. Deser and M. Alexander and from the French Programme National d'Etude du Climat to G. Reverdin. The graphics were produced with the GrADS software package developed by Brian Doty. We thank Michael Alexander and three anonymous reviewers for helpful comments.

References

Agnew, T., Simultaneous winter sea-ice and atmospheric circulation anomaly patterns, *Atmos. Ocean*, *31*, 259–280, 1993.

Belkin, I. M., S. Levitus, J. I. Antonov, and S.-A. Malmberg, "Great Salinity Anomalies" in the North Atlantic, *Prog. Oceanogr.*, *41*, 1–68, 1998.

Bhatt, U. S., M. A. Alexander, D. S. Battisti, D. D. Houghton, and L. M. Keller, Atmosphere-ocean interaction in the North Atlantic: Near-surface variability, *J. Clim.*, *11*, 1615–1632, 1998.

Bishop, J. K. B., W. B. Rossow, and E. G. Dutton, Surface solar irradiance from the international satellite cloud climatology project 1983–1991, *J. Geophys. Res.*, *102*, 6883–6910, 1997.

Bitz, C. M., and W. H. Lipscomb, An energy-conserving thermodynamic model of sea ice, *J. Geophys. Res.*, *104*, 15,669–15,677, 1999.

Bitz, C. M., M. M. Holland, M. Eby, and A. J. Weaver, Simulating the ice-thickness distribution in a coupled climate model, *J. Geophys. Res.*, *106*, 2441–2463, 2001.

Chapman, W. L., and J. E. Walsh, Recent variations of sea ice and air temperature in high latitudes, *Bull. Am. Meteorol. Soc.*, *74*, 33–47, 1993.

Deser, C., and M. Blackmon, Surface climate variations over the North Atlantic Ocean during winter: 1900–1989, *J. Clim.*, *6*, 1743–1753, 1993.

Deser, C., and M. S. Timlin, *Decadal Variations in Sea Ice and Sea Surface Temperature in the Subpolar North Atlantic: Proceedings of the Atlantic Climate Change Program Principal Investigators Meeting,* edited by A.-M. Wilburn, Woods Hole Oceanogr. Inst., Woods Hole, Mass., 1996.

Deser, C., J. E. Walsh, and M. S. Timlin, Arctic sea ice variability in the context of recent atmospheric circulation trends, *J. Clim.*, *13*, 617–633, 2000a.

Deser, C., M. A. Alexander, and M. S. Timlin, Re-emergence of winter SST anomalies in the North Atlantic: 2000 U.S. WOCE report, *U.S. WOCE Implement. Rep.12*, 60 pp., U.S. WOCE Off., College Station, Tex., 2000b.

Dickson, R. R., J. Meincke, S.-A. Malmberg, and A. J. Lee, The "Great Salinity Anomaly" in the northern North Atlantic, 1968–1982, *Prog. Oceanogr.*, *20*, 103–151, 1988.

Fang, Z., and J. M. Wallace, Arctic sea ice variability on a timescale of weeks: Its relation to atmospheric forcing, *J. Clim.*, *7*, 1897–1913, 1994.

Hahn, C. J., S. G. Warren, J. London, R. L. Jenne, and R. M. Chervin, Climatological data for clouds over the globe from surface observations, *Rep. NDP-026*, 56 pp., Carbon Dioxide Inf. Cent., Oak Ridge, Tenn., 1987.

Hibler, W. D., A dynamic thermodynamic sea ice model, *J. Phys. Oceanogr.*, *9*, 815–846, 1979.

Houghton, R. W., Subsurface quasi-decadal fluctuations in the North Atlantic, *J. Clim.*, *9*, 1363–1373, 1996.

Hunke, E. C., and J. K. Dukowicz, An elastic-viscous-plastic model for sea ice dynamics, *J. Phys. Oceanogr.*, *27*, 1849–1867, 1997.

Ikeda, M., Decadal oscillations of the air-ice-ocean system in the Northern Hemisphere, *Atmos. Ocean*, *28*, 106–139, 1990.

Ikeda, M., T. Yao, and G. Symonds, Simulated fluctuations in annual Labrador Sea ice cover, *Atmos. Ocean*, *26*, 16–39, 1988.

Kalnay, E., et al., The NCEP/NCAR reanalysis project, *Bull. Am. Meteorol. Soc.*, *77*, 437–471, 1986.

Large, W. G., G. Danabasoglu, S. C. Doney, and J. C. McWilliams, Sensitivity to surface forcing and boundary layer mixing in a global ocean model: Annual-mean climatology, *J. Phys. Oceanogr.*, *27*, 2418–2447, 1997.

Marko, J. R., D. B. Fissel, P. Wadhams, P. M. Kelly, and R. D. Brown, Iceberg severity off eastern North America: Its relationship to sea ice variability and climate change, *J. Clim.*, *7*, 1335–1351, 1994.

Marsden, R. F., L. A. Mysak, and R. A. Myers, Evidence for stability enhancement of sea ice in the Greenland and Labrador Seas, *J. Geophys. Res.*, *96*, 4783–4789, 1991.

Mysak, L. A., and D. K. Manak, Arctic sea ice extent and anomalies, 1953–1984, *Atmos. Ocean*, *27*, 376–405, 1989.

Mysak, L. A., D. K. Manak, and R. F. Marsden, Sea ice anomalies observed in the Greenland and Labrador Seas during 1901–1984 and their relation to an interdecadal Arctic climate cycle, *Clim. Dyn.*, *5*, 111–133, 1990.

Mysak, L. A., R. G. Ingram, J. Wang, and A. Van Der Baaren, The anomalous sea-ice extent in Hudson Bay, Baffin Bay and the Labrador Sea during three simultaneous ENSO and NAO episodes, *Atmos. Ocean*, *34*, 313–343, 1996.

Parkinson, C. L., D. J. Cavalieri, P. Gloersen, H. J. Zwally, and J. Comiso, Arctic sea ice extents, areas and trends, 1978–1996, *J. Geophys. Res.*, *104*, 20,837–20,856, 1999.

Prinsenberg, S. J., I. K. Peterson, S. Narayanan, and J. U. Umoh, Interaction between atmosphere, ice cover and ocean off Labrador and Newfoundland from 1962–1992, *Can. J. Aquat. Sci.*, *54*, 30–39, 1997.

Reverdin, G., D. Cayan, and Y. Kushnir, Decadal variability of hydrography in the upper northern North Atlantic in 1948–1990, *J. Geophys. Res.*, *102*, 8505–8531, 1997.

Rogers, J., C.-C. Wang, and M. J. McHugh, Persistent cold climatic episodes around Greenland and Baffin Island: Links to decadal-scale sea surface temperature anomalies, *Geophys. Res. Lett.*, *25*, 3971–3974, 1998.

Rossow, W. B., and R. A. Schiffer, ISCCP cloud data products, *Bull. Am. Meteorol. Soc.*, *27*, 2–20, 1991.

Slonosky, V. C., L. A. Mysak, and J. Derome, Linking arctic sea ice and atmospheric circulation anomalies on interannual and decadal time scales, *Atmos. Ocean*, *35*, 333–366, 1997.

Smith, R. D., J. K. Dukowicz, and R. C. Malone, Parallel ocean circulation modeling, *Physica D*, *60*, 38–61, 1992.

Taylor, A. H., and J. A. Stephens, Seasonal and year-to-year variations in surface salinity at the nine North Atlantic Ocean weather stations, *Oceanol. Acta*, *3*, 421–430, 1980.

Trenberth, K. E., Some effects of finite sample size and persistence on meteorological statistics, part I, Autocorrelations, *Mon. Weather Rev.*, *112*, 2359–2368, 1984.

Trenberth, K. E., and D. A. Paolino, The Northern Hemisphere sea-level pressure data set: Trends, errors and discontinuities, *Mon. Weather Rev.*, *108*, 855–872, 1980.

Walsh, J. E., and C. M. Johnson, An analysis of arctic sea ice fluctuations, 1953–1977, *J. Phys. Oceanogr.*, *9*, 580–591, 1979.

Watanabe, M., and M. Kimoto, On the persistence of decadal SST anomalies in the North Atlantic, *J. Clim.*, *13*, 3017–3028, 2000.

Woodruff, S. D., R. J. Slutz, R. L. Jenne, and P. M. Steurer, A comprehensive atmosphere-ocean data set, *Bull. Am. Meteorol. Soc.*, *68*, 1239–1250, 1987.

Xie, P., and P. A. Arkin, Analyses of global monthly precipitation using gauge observations, satellite estimates, and numerical model predictions, *J. Clim.*, *9*, 840–858, 1996.

C. Deser and M. Holland, Climate and Global Dynamics Division, NCAR, PO Box 3000, Boulder, CO 80307-3000, USA. (cdeser@ucar.edu)

G. Reverdin, Laboratoire d'Etudes in Géophysique et Océnographie Spatiales (LEGOS), GRGS, CNES, 14 Av. E. Belin, 31401 Toulouse Cx 4, France.

M. Timlin, NOAA-CIRES Climate Diagnostics Center, R/CDC1, 325 Broadway, Boulder, CO 80305, USA.